

Evolution with size in a locally periodic system: scattering and deterministic maps

V Domínguez-Rocha and M Martínez-Mares

Departamento de Física, Universidad Autónoma Metropolitana-Iztapalapa, Apartado Postal 55-534, 09340 México Distrito Federal, Mexico

E-mail: vdr@xanum.uam.mx, moi@xanum.uam.mx

Abstract. In this paper we study the evolution of the wave function with the system size in a locally periodic structure. In particular we analyse the dependence of the wave function with the number of unit cells, which also reflects information about its spatial behaviour in the system. We reduce the problem to a nonlinear map and find an equivalence of its energy regions of single periodicity and of weak chaos, with the forbidden and allowed bands of the fully periodic system, respectively. At finite size the wave function decays exponentially with system size, as well as in space, when the energy lies inside a region of single periodicity, while for energies in the weak chaotic region never decays. At the transition between those regions the wave function still decays but in a q -exponential form; we found that the decay length is a half of the mean free path, which is larger than the lattice constant.

PACS numbers: 05.60.Gg, 05.45.Ac, 72.10.-d, 72.20.Dp

1. Introduction

Crystalline materials occupy a special place in the solid state physics. Despite that in real life the majority of the solids are non crystalline, crystals help to understand a lot of the properties of the solid matter. At the macroscopic scale crystalline solids are considered as infinite periodic systems, which are well described by the band theory [1]. However, the propagation of electrons through a locally periodic system, which consists of a finite number N of repeating elements [2], has been of great interest due to the practical applications in designing artificial materials with specific features. That is the case of layered periodic structures or finite superlattices [3, 4, 5], and man-made devices fabricated with optical lattices to model condensed matter systems [6, 7, 8, 9, 10]. Furthermore, the applicability of locally periodic structures cover a wide range that includes structurally chiral materials [11]; microwave [12], photonic [13, 14, 15], and phononic [16, 17] crystals, as well as elastic or acoustic systems [18, 19, 20].

The study of locally periodic structures is mainly concerned with the band formation for several cases of fixed N , where each one is analysed separately to look for the emergence of the allowed and forbidden bands [21, 22, 23, 24]. In all cases, precursors of the band structure of the corresponding fully periodic system, which is almost formed when N is large enough, can be observed [2]. An interesting question that immediately arises is how or when the properties of a fully periodic systems are reached. Of course, the standard method of band theory for crystals is not applicable for finite systems. Therefore, to answer this question it is necessary to study the evolution of the system as N increases. This procedure allows to get additional information about the band formation; that is, the evolution to the infinite system should not be the same for energies in the gap than those in an allowed band of the fully periodic system.

Along this line, the electronic transport on a double Cayley tree was studied as a function of the generation, which plays the same role as N [25]. There, a remarkable equivalence between the electronic transport and the dynamics of an intermittent low-dimensional nonlinear map has been exhibited; the map presents regions of weak chaos and of single periodicity, whose Lyapunov exponents are zero and negative, which indicates the conducting and insulating phases, respectively [26]. The conductance oscillates with the generation in the weakly chaotic attractors of the map, indicating conducting states. In the attractors of single periodicity, the conductance decays exponentially as is typical for insulating states, but at the transition the intermittency of the map makes the conductance to reach the insulating phase in a q -exponential form. Therefore, there exist typical length scales on the different energy regions that remain to be understood.

A scaling analysis of the conductance is one way to obtain information about the metallic or insulating behaviour of a system [27]. But, the conductance is a global quantity and not much can be said about the local character in the system. Therefore, it is important to study the wave function directly, whose spatial behaviour should reflect whether a system behaves as a conductor or not.

The purpose of the present paper is to analyse the evolution of the wave function with N and once this is done, look at its spatial behaviour in a locally periodic structure in one dimension. This study allows to determine the nature of the several states in the system, to answer the question posted above, and to find a physical interpretation of the typical lengths scales in the problem. In order to do this, we consider a locally periodic potential that is formed by a sequence of individual scattering potentials. For our purpose, it is not necessary to consider an open system on both edges. Therefore, without any loss of generality, we avoid unnecessary complications and restrict the system to have only one entrance. We solve the problem analytically for arbitrary individual potentials using the scattering matrix formalism. Following the same ideas of reference [25] we reduce the problem to the analysis of the dynamics of an intermittent low-dimensional nonlinear map.

We organize the paper as follows. In the next section we present the scattering approach to our linear chain of scatterers. In the same section, the recursive relation satisfied by the scattering matrix, when an individual scatterer is added, is reduced to a nonlinear map. The scaling analysis and the spatial dependence of the wave function is presented in section 3. We present our conclusions in section 4.

2. A serial structure of quantum scatterers

2.1. Scattering approach

The quantum system that we consider is a one-dimensional locally periodic whose separation between adjacent scatterers is a , that we will refer to it as the lattice constant. This chain consists of N identical scatterers, each one described by the potential $V_b(x)$ of arbitrary shape and range b , as shown in figure 1. The unit cell consists of a free region of size $a - b$ plus the potential of range b , except in the first one where the size of the free region is $a - b/2$. Our chain lies in the semispace at the right of the origin, bounded on the left ($x = 0$) by a potential step of high $V_0 \gg E$, where E is the energy of the quantum particle; the right side of the chain remains open. We assume that each scatterer is described by a unitary scattering matrix S_b that has the following structure:

$$S_b = \begin{pmatrix} r_b & t'_b \\ t_b & r'_b \end{pmatrix}, \quad (1)$$

where r_b (r'_b) and t_b (t'_b) are the reflection and transmission amplitudes for incidence on the left (right) of the potential, respectively.

As we will see below, the evolution of several properties of the system with the number of scatterers can be obtained from the scattering matrix of the system. Therefore, we write the scattering matrix S_N , that describes the system with N scatterers, in terms of the one with $N - 1$ of them, S_{N-1} , by adding an individual scatterer using the combination rule of scattering matrices. The combination of S_{N-1}

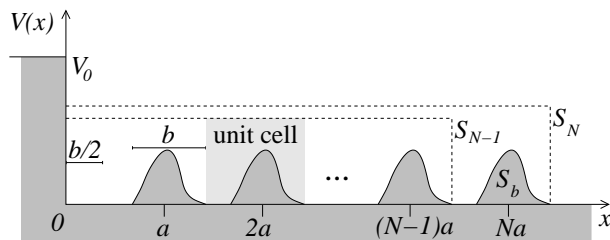


Figure 1. A serial structure of identical scatterers, each one represented by a potential V_b of arbitrary shape and range b , whose associated scattering matrix is S_b . The chain is bounded on the left side by a potential step and opened on the right side.

and S_b gives the following recursive relation, namely

$$S_N = r'_b + t_b \frac{1}{e^{-2ik(a-b)} - S_{N-1}r_b} S_{N-1}t'_b, \quad (2)$$

where $k = \sqrt{2ME/\hbar^2}$, with M the mass of the particle. The initial condition for this recursive relation is the scattering matrix S_0 associated to the scattering due to the potential step but measured at $x = b/2$.

2.2. Reduction to a nonlinear map

Since S_N relates the amplitude of the outgoing plane wave to the amplitude of the incoming one to the system, it is a 1×1 unitary matrix that can be parameterized just by a phase, θ_N , as

$$S_N = e^{i\theta_N}. \quad (3)$$

The recursive relation (2) can be seen as a one-dimensional nonlinear map. That is, $\theta_N = f(\theta_{N-1})$, where

$$f(\theta_{N-1}) = -\theta_{N-1} + 2 \arctan \frac{\text{Im}(r'_b \alpha_b^* + \alpha_b e^{i\theta_{N-1}})}{\text{Re}(r'_b \alpha_b^* + \alpha_b e^{i\theta_{N-1}})}, \quad (4)$$

modulo π . Here, $\alpha_b = t_b e^{i\phi/2} e^{ik(a-b)}$, $e^{i\phi} = t'_b/t_b$, and $\text{Re}(\alpha')$ and $\text{Im}(\alpha')$ denote the real and imaginary parts of α' . Because the reflected wave at the potential step acquires an additional phase θ_{step} , then $S_0 = e^{i\theta_0}$ where $\theta_0 = \theta_{\text{step}} + kb$, which is the initial condition for the map.

Although the nonlinear map (4) is valid for arbitrary individual potentials, it is necessary to consider a particular case to look for the characteristics of the map. Let us assume for a moment that an individual potential is just a delta potential of intensity v and null range, $b = 0$. In this case, $r_b = r'_b = -u/(u - 2ik)$ and $t_b = t'_b = -2ik/(u - 2ik)$, where $u = 2Mv/\hbar^2$ [28]. The corresponding bifurcation diagram is shown in figure 2 (a), from which we observe ergodic windows between windows of periodicity one. The width of an ergodic window depends on the potential intensity, as well as on the energy; it becomes wider when ka increases (when referring to the delta potential we will speak of ka instead of k), as it is expected since for higher energies, smaller the effect of the

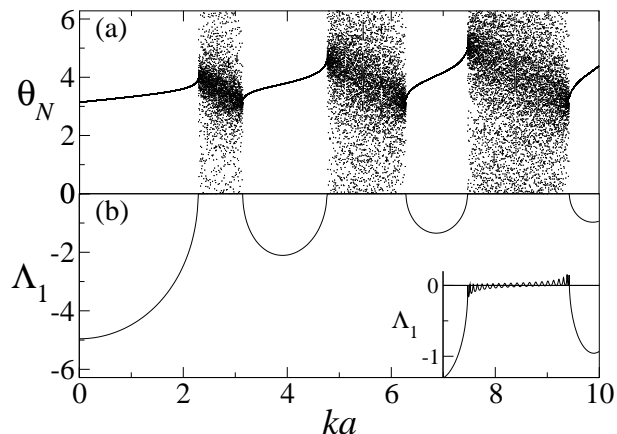


Figure 2. (a) Bifurcation diagram for a chain of delta potentials with $ua = 10$. We plot only the last thirty iterations of $N = 1000$ for the phase as a function of ka starting with an initial condition $\theta_0 = \pi$. We also plot the analytical results given by Eqs. (12) and (17) but they are indistinguishable from the numerics. (b) Finite N Lyapunov exponent $\Lambda_1(N)$ as a function of ka for $N = 1000$. Theoretical result λ_1 given by (22) is also plotted; it is indistinguishable from $\Lambda_1(N)$ for very large N . Inset: Λ_1 for $N = 20$.

potential. In the ergodic window θ_N fluctuates, while in the window of periodicity one it reaches a fixed value when N is very large.

Figure 2 (a) suggests that, in a window of periodicity one, (2) reaches a fixed point solution for S_N of the form shown in (3), for very large N . If we look for it, we find a stable and an unstable fixed point solutions, $e^{i\theta_{\pm}}$ [see figure 3 (a)]. In an ergodic window, (2) does not have solution of the form (3), but of the form $w_{\pm} = |w_{\pm}|e^{i\theta}$, being θ the value around which θ_N fluctuates with an invariant density. We will see below that these fixed point solutions are marginally stable [29]. The stable and marginally stable fixed point solutions can be summarized as

$$S_{\infty} = \begin{cases} e^{i\theta_+} & \text{for } k'_{c_{m-1}} < k < k_{c_m} \\ w_{\pm} & \text{for } k_{c_m} < k < k'_{c'_m} \\ e^{i\theta_-} & \text{for } k'_{c'_m} < k < k_{c_{m+1}} \end{cases}, \quad (5)$$

where k_{c_m} and $k'_{c'_m}$ denote the critical values of k on the left and right edges of the corresponding ergodic window [see (10) below];

$$e^{i\theta_{\pm}} = \frac{1}{r'_b \alpha_b} \left[\pm \sqrt{(\text{Re } \alpha_b)^2 - |t_b|^4} + i \text{Im } \alpha_b \right] \quad (6)$$

for $|\text{Re } \alpha_b(k)| > |t_b(k)|^2$ and

$$w_{\pm} = \frac{i}{r'_b \alpha_b} \left[\pm \sqrt{|t_b|^4 - (\text{Re } \alpha_b)^2} + \text{Im } \alpha_b \right] \quad (7)$$

for

$$|\text{Re } \alpha_b(k)| \leq |t_b(k)|^2, \quad (8)$$

such that

$$\tan \theta = \frac{\text{Im}(ir'_b \alpha_b^*)}{\text{Re}(ir'_b \alpha_b^*)}. \quad (9)$$

The equality in (8) determines the critical values k_{c_m} and $k_{c'_m}$; that is

$$|\text{Re} \alpha_b(k_c)| = |t_b(k_c)|^2, \quad (10)$$

where k_c denotes k_{c_m} or $k_{c'_m}$. At a critical attractor, θ takes the value $\theta(k_c) = \theta_c$, where

$$\tan \theta_c = \frac{\text{Im}[ir'_b(k_c) \alpha_b^*(k_c)]}{\text{Re}[ir'_b(k_c) \alpha_b^*(k_c)]}. \quad (11)$$

The condition (8) is equivalent to that for allowed bands in the infinite linear chain of scatterers [30]. Therefore, we have found a correspondence between windows of single periodicity (or chaotic) and forbidden (or allowed) bands in the limit $N \rightarrow \infty$, in a similar way as happens for the double Cayley tree studied in Ref. [25]. Equation (10) defines the left and right edges of the chaotic windows.

The dynamics of the map is expected to be different on each type of windows of the bifurcation diagram. To observe the trajectories on each region of k we need to back to the particular case of delta potentials. For this case, (6) gives

$$e^{i\theta_{\pm}} = -i \frac{2ka}{ua} e^{-ika} [\pm x(ka) + i y(ka)], \quad (12)$$

where

$$\begin{aligned} x(ka) &= \sqrt{\left(\cos ka + \frac{ua}{2ka} \sin ka\right)^2 - 1} \\ y(ka) &= \sin ka - \frac{ua}{2ka} \cos ka \end{aligned} \quad (13)$$

for $|\cos ka + (ua/2ka) \sin ka| > 1$, while (7) gives

$$w_{\pm} = \frac{2ka}{ua} e^{-ika} [\pm x'(ka) + y(ka)], \quad (14)$$

where

$$x'(ka) = \sqrt{1 - \left(\cos ka + \frac{ua}{2ka} \sin ka\right)^2} \quad (15)$$

for

$$\left|\cos ka + \frac{ua}{2ka} \sin ka\right| \leq 1, \quad (16)$$

which is the condition for allowed bands in the Kronig-Penney model [31]. From (14) it is easy to see that the phase of w_{\pm} is given by [see (9)]

$$\theta = -ka + (m+1)\pi, \quad m = 0, 1, \dots \quad (17)$$

The band edges are obtained from the equality in (16), namely

$$\tan \frac{k_{c_m} a}{2} = \begin{cases} ua/2k_{c_m} a, & \text{for } m \text{ odd} \\ -2k_{c_m} a/ua, & \text{for } m \text{ even} \end{cases}, \quad (18)$$

and $k_{c'_m} a = m\pi$, for m odd and even. At the band edges, $\theta(k_{c_m} a) = \theta_{c_m}$, with $\theta_{c_m} = -k_{c_m} a + (m+1)\pi$. For the first chaotic window ($m = 1$), $k_{c_1} a = 2.28445 \dots$

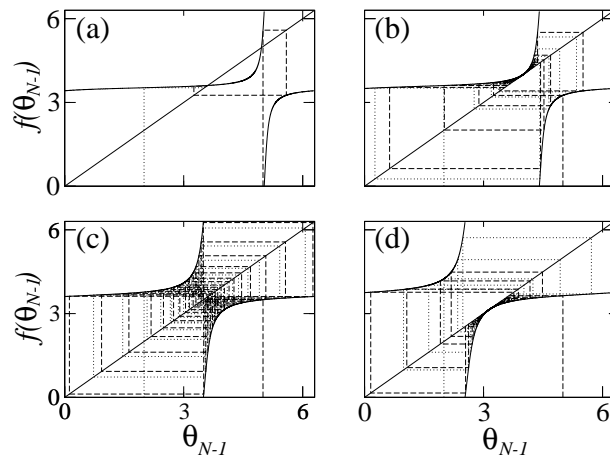


Figure 3. Dynamics of the map (4) applied to the delta potential, where $ua = 10$ and ka taking the values (a) 2, (b) 2.2846, (c) 2.8, and (d) 3.14145. Each panel shows the trajectories for initial conditions $\theta_0 = 2$ and 5.

and $k_{c_1}a = \pi$, $\theta_{c_1} = 3.99873\dots$, and $\theta_{c_1} = \pi$. Equations (12) and (17) coincide with the numerical results in both sides and inside of the first chaotic window, as it is shown in figure 2 (a).

The trajectories of the map for this example are shown in figure 3 for some values of ka . In panel (a) $ka = 2$, ka is inside the window of period one; we observe that all trajectories (we show only two) converge to a fixed point as $N \rightarrow \infty$, which corresponds to $\theta_+ \approx 3.61$. Panels (b) and (d) show intermittent trajectories at the tangent bifurcations when $ka = 2.2846$ and 3.14145 , very close to the transitions from the chaotic side. In panel (c), deep inside the chaotic window, the trajectories never converge. Therefore, we observe that the behaviour of the trajectories for two initial conditions strongly depends on the specific region to which ka belongs. The dynamics of the map can be analysed by means of the sensitivity to initial conditions, something that we do next.

2.3. Sensitivity to initial conditions

The dynamics of the nonlinear map (4) is characterized by the sensitivity to initial conditions. For finite N it is defined by [25]

$$\Xi_N \equiv \left| \frac{d\theta_N}{d\theta_0} \right| \equiv e^{N\Lambda_1(N)}, \quad (19)$$

where θ_0 is the initial condition and $\Lambda_1(N)$ is the finite N Lyapunov exponent, whose dependence on N is shown as an argument (the subscript 1 will be clear below). For the map (4), Ξ_N satisfies the following recursive relation:

$$e^{N\Lambda_1(N)} = \frac{|t_b|^4}{|r'_b \alpha_b^* + \alpha_b S_{N-1}|^2} e^{(N-1)\Lambda_1(N-1)}. \quad (20)$$

In figure 2 (b) we plot $\Lambda_1(N)$ obtained from (20) for the delta potentials as a function of ka , for $N = 1000$. We observe that $\Lambda_1(N)$ is negative in the windows of period one, indicating that Ξ_N decays exponentially with N when N is very large. This means that any trajectory in the map converges rapidly to a fixed point, as happens in figure 3 (a). In the chaotic windows, $\Lambda_1(N)$ goes to zero in the limit $N \rightarrow \infty$. There, Ξ_N does not depend on N and nothing can be said about the convergence of any trajectory; this situation corresponds to figure 3 (c). For a finite number of iterations $\Lambda_1(N)$ is still negative in the windows of period one, but it oscillates around zero in the chaotic windows. This can be seen in the inset of figure 2; the amplitude of those oscillations tend to zero as N increases; this is a signal of weak chaos [26, 32]. Here, we are interested in the behaviour of Ξ_N with N .

With this evidence, we can assume that, in the limit $N \rightarrow \infty$, $\Lambda_1(N) \rightarrow \lambda_1$ and $\Xi_N \rightarrow \xi_N$, where ξ_N is the sensitivity to initial conditions defined by

$$\xi_N = e^{N\lambda_1}, \quad (21)$$

where λ_1 is the Lyapunov exponent of the map, which is given by

$$\lambda_1 = \ln \frac{|t_b|^4}{|r'_b \alpha_b^* + \alpha_b S_\infty|^2}. \quad (22)$$

For one of the two roots expressed in (6), which are valid for k in a window of period one, λ_1 is positive. This means that the fixed point solution is unstable. The second solution is a stable one since λ_1 is negative. It is the last one, the only that appears in figure 2 (a). In the chaotic windows there are two values of λ_1 that correspond to the two solutions w_\pm , one positive and another negative, both at the same distance from zero. We find that the Lyapunov exponent that agrees with $\Lambda_1(N)$, which has been obtained iteratively for very large N , is the average of those values, which is zero. In figure 2 (b) we compare λ_1 of (22) with $\Lambda_1(N)$ calculated iteratively by means of (20), for the delta potentials. For $N = 1000$ we observe that both results are indistinguishable. Therefore, (21) says that ξ_N decays exponentially with N for k in the windows of period one and remains constant in the chaotic windows. These results are verified in panels (a) and (c) of figure 4, where we compare (21) with the numerical calculations for the delta potential.

The behaviour of the sensitivity to initial conditions is very different at the critical attractors, since there an anomalous dynamics occurs due to the tangent bifurcation [33, 34]. A critical attractor is located at the point (k_c, θ_c) , where k_c denotes k_{c_m} or $k'_{c'_m}$ and θ_c , θ_{c_m} or $\theta'_{c'_m}$. If we make an expansion of θ_N close to θ_c the result is given by

$$\theta_N - \theta_c = (\theta_{N-1} - \theta_c) + u(\theta_{N-1} - \theta_c)^z + \dots, \quad (23)$$

where $z = 2$ and $u = \mp |r'_b(k_c)|^2$. From known properties of this nonlinearity of the tangent bifurcation, the sensitivity obeys a q -exponential law for large N [34]. That is, $\Xi_{N \rightarrow \infty} = \xi_N$, where

$$\xi_N \propto e_q^{N\lambda_q} \equiv [1 - (q-1)N\lambda_q]^{-1/(q-1)}, \quad (24)$$

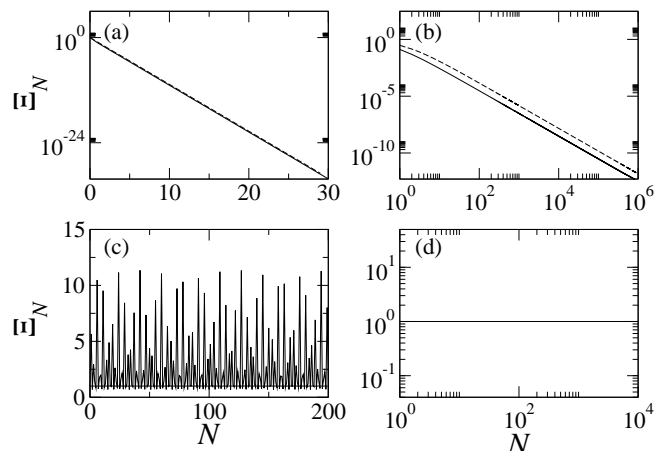


Figure 4. The continuous lines represent the result for the sensitivity to initial conditions for finite N , Ξ_N , as a function of N for the chain of delta potentials with $ua = 10$ and ka equal to (a) 2, (b) 2.28445..., (c) 2.8, and (d) 3.14145. The dashed lines are the theoretical results given by (21) for (a) and (c), and (24) for (b). In (d) ξ_N remains constant with N .

with $q = 1 - 1/z = 3/2$ and $\lambda_{3/2} = zu = \mp 2|r'_b(k_c)|^2$. The minus and plus signs correspond to trajectories at the left and right (right and left) of the point of tangency $\theta_c = \theta_{c_m}$ ($\theta_c = \theta'_{c_m}$), respectively; that is, ξ_N decays with N with a power law when $\theta_{N-1} - \theta_{c_m} < 0$ ($\theta_{N-1} - \theta'_{c_m} > 0$) and grows faster than exponential when $\theta_{N-1} - \theta_{c_m} > 0$ ($\theta_{N-1} - \theta'_{c_m} < 0$).

In panels (b) and (d) of figure 4 we show the behaviour of Ξ_N with N at the edges $k_{c_1}a$ and $k'_{c_1}a$, obtained from the numerical calculation for the delta potential, and compare them with (24). In (b) it is clear that Ξ_N behaves as ξ_N of (24) at $ka = k_{c_1}a$ for very large N . That is not the case at the right edge $ka = k'_{c_1}a$ where Ξ_N remains constant with N . This pathological behaviour is because $k'_{c_1}a$ corresponds to a resonance and the nodes the delta potentials become invisible.

3. Behaviour of the wave function

3.1. Evolution of the wave function with the system size

The wave function in the region between the individual potentials can be written as a superposition of plane waves traveling to the left and right. If we normalize it, in such a way that the amplitude after the last scatterer is one, the square modulus of the wave function in the region between the scatterers n and $n+1$, labeled by n ($n = 0, 1, \dots, N$), can be written as

$$|\psi_n^{(N)}(x)|^2 = \frac{e_q^{N\Lambda_q(N)}}{e_q^{n\Lambda_q(n)}} \cos^2 [k(x - na - b/2) + \theta_n/2], \quad (25)$$

where $q = 1$ for k in the windows of single period and of weak chaos; $q = 3/2$ at the transition from the chaotic side. We see from (25) that at the position x , the amplitude

of the wave function depends on N only through the numerator. This means that we can replace N by $N - 1$ to find the wave function at the same position for a chain made of $N - 1$ scatterers. Hence, the following recursive relation is satisfied by the square modulus of the wave function:

$$|\psi_n^{(N)}(x)|^2 = \frac{e_q^{N\Lambda_q(N)}}{e_q^{(N-1)\Lambda_q(N-1)}} |\psi_n^{(N-1)}(x)|^2. \quad (26)$$

An iteration process lead us to

$$|\psi_n^{(N)}(x)|^2 = e_q^{N\Lambda_q(N)} |\psi_n^{(0)}(x)|^2, \quad (27)$$

where $\psi_n^{(0)}(x)$ is the wave function at x in the absence of any scatterer.

The factor in front of the right hand side of (27) is just the sensitivity to initial conditions for finite N [see (19)]. Therefore, the evolution of $|\psi_n^{(N)}(x)|^2$ with N is given by Ξ_N , as shown in figure 4. This evolution resemble the behaviour of the conductance in a double Cayley tree with system size [25]. For energies in a window of period one, $|\psi_n^{(N)}(x)|^2$ decays exponentially with N , for $N \gg 1$, with a typical decay length which we identify with a localization length due to the similar scaling behaviour of the conductance with N [25]; this localization length is given by

$$\zeta_1 = \frac{a}{|\lambda_1|}. \quad (28)$$

When $|\lambda_1| > 1$, on the one hand, the localization length is smaller than the lattice constant; this occurs far from the transition to the chaotic side; close to the transition $\zeta_1 > a$. On the other hand, for energies in the chaotic window, $|\psi_n^{(N)}(x)|^2$ never decays but oscillates as N increases; there, $\lambda_1 = 0$ such that a localization length can not be defined. However, at the transition from the chaotic side the wave function shows a power law decay with N [see figure 4(b)]. The typical decay length, that we identify with a localization length too, is given by

$$\zeta_{3/2} = \frac{a}{|\lambda_{3/2}|} = \frac{a}{2|r'_b(k_c)|^2}. \quad (29)$$

What is very interesting here is that the term on the right hand side of the second equality is $\ell/2$, where

$$\ell = \frac{a}{|r'_b(k_c)|^2}, \quad (30)$$

which is a definition of the mean free path [35, 36]. This equation means that the mean free path is larger than the lattice constant. This result is in agreement with the one obtained from Esaki and Tsu, where $\ell \sim 3a$, in a superlattice [37]. For our particular case of a delta potential with $ua = 10$, $\ell \approx 1.21a$ for $k_{c_1}a = 2.28445\dots$, and $\ell \approx 1.4a$ for $k_{c_1}a = \pi$. The behaviour of the wave function in the space can let us to understand the nature of the states on the different energy regions.

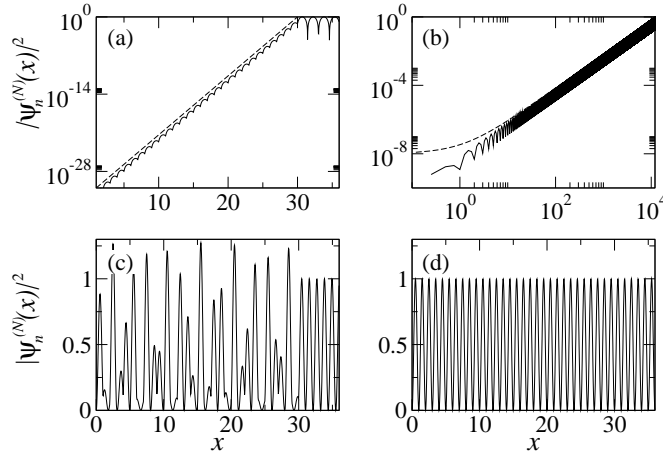


Figure 5. Square of the wave function as a function of x for the chain of delta potentials with $ua = 10$. In (a) we compare (32) (continuous line) with an exponential with localization length given by (28) (dashed line), for $ka = 2$. In (b) we compare (33) (continuous line) with a q -exponential decay with localization length given by (29) (dashed line), for $ka = 2.28445\dots$ (c) For $ka = 2.8$ the wave function is extended. In (c) the system is invisible at a resonance at $ka = \pi$.

3.2. Spatial behaviour of the wave function

In the limit of very large N , $\Lambda_q(N) \rightarrow \lambda_q$ and the squared modulus of the wave function given by (25) can be written as

$$|\psi_n^{(N)}(x)|^2 = \frac{e_q^{N\lambda_q}}{e_q^{n\lambda_q}} \cos^2 [k(x - na - b/2) + \theta_n/2]. \quad (31)$$

For k far from the critical attractors, $q = 1$ and the ordinary exponential function is recovered. In this case the spatial behaviour of the wave function is given by

$$|\psi_n^{(N)}(x)|^2 = e^{-(N-n)a/\zeta_1} \cos^2 [k(x - na - b/2) + \theta_n/2]. \quad (32)$$

This equation means that when the energy is in a window of period one, the wave function decreases exponentially in space from the boundary ($n = N$) to inside of the system ($n < N$). In this case the quantum particle is spread over few ζ_1 's. It is in this sense that we interpret ζ_1 as a localization length. This localization length is smaller than the period of our locally periodic structure, a , except very close to the transition region. This situation is illustrated in figure 5 (a) for the chain of delta potentials.

For energies in the weakly chaotic windows $\zeta_1 \rightarrow \infty$ and the wave function becomes extended through the system, as can be seen in figure 5 (c).

Near the transition, at the weakly chaotic attractors, (31) can be written as

$$|\psi_n^{(N)}(x)|^2 = \left(\frac{1 \pm na/2\zeta_{3/2}}{1 \pm Na/2\zeta_{3/2}} \right)^2 \cos^2 [k(x - na - b/2) + \theta_n/2], \quad (33)$$

where we used that $\lambda_{3/2} = \mp a/\zeta_{3/2}$. The plus (minus) sign in (33) corresponds to the left (right) chaotic attractor. This equation clearly shows a power law decay from

the boundary. That is, the wave function is still localized but the localization is not exponential, but q -exponential. It is interesting to note that the localization length is $\zeta_{3/2} = \ell/2$. The factor 1/2 is due to the fact that the localization length is measured from the maximum of the wave function, which in this case is at the boundary of the system, while the mean free path implicitly assumes the width of a wave packet; according to Esaki and Tsu [37], the mean free path in a superlattice is the uncertainty in the position. In figure 5 (b) we can observe the power law decay of the squared modulus of the wave function for the chain of delta potentials. Figure 5 (d) shows the behaviour of the squared modulus of the wave function at the attractor on the right side of the chaotic window. In this case, the system is invisible since $k_{c1}a = \pi$ corresponds to a resonance and the wave function has nodes just at the delta potentials.

4. Conclusions

We considered a locally periodic structure in one dimension, which consists of a chain of potentials of arbitrary shape. We studied the evolution of the wave function of the chain when the system size increases. This procedure helped us to observe the behaviour of the wave function in space when the size of the system remains fixed.

Since the system is not fully periodic, we can not use the traditional band theory. Instead of that we take advantage of a recursion relation of the scattering matrix, in terms of the number of scatterers, to reduce the problem to a nonlinear map. Through this method all information about the behaviour of the system was obtained from the dynamics of this map. In this way we could understand how and when the band theory of the fully periodic chain is reached by the knowledge of the type of evolution of the wave function with the system size. We found an equivalence between the periodic and weakly chaotic regions of the map and the forbidden and allowed bands, respectively. This equivalence is similar to that remarked in the literature for the conductance of a double Cayley tree, where it is null in the windows of period one, and oscillates in regions of weak chaos. Also, we found that the wave function at a given position scales with the system size in a similar way as the conductance does. In a window of period one, far from the transition to the chaotic window, the wave function decays exponentially with a typical length scale, which is smaller than the lattice constant. Very close to the transition from the window of period one, this typical length becomes larger than the lattice constant. This behaviour driven us to interpret the typical scale as a localization length. We corroborated this interpretation by the exponential localization of the wave function close to the boundary of the finite system. In the chaotic region the wave function does not decay and a localization length can not be defined.

At the transition between periodic and weakly chaotic regions, but from the chaotic side, the wave function scales as a power law. This implies that it is still localized but with a q -exponential form. The localization length were found to be one half of the mean free path. We demonstrate analytically, that the mean free path is larger than the lattice constant, in complete agreement with a result found in the literature for a

supperlattice.

Finally, it is worth mentioning that our development considers independent quantum particles such that classical waves can also be used. In particular, one-dimensional elastic systems are strong candidates to simulate our quantum system by means of elastic rods with narrow notches [19].

Acknowledgments

The authors thank RA Méndez-Sánchez and G Báez useful discussions. M Martínez-Mares is grateful with the Sistema Nacional de Investigadores, Mexico, and with MA Torres-Segura for her encouragement. V Domínguez-Rocha thanks financial support from CONACyT, Mexico, and partial support from C Jung through the CONACyT project No. 79988.

- [1] Ashcroft N W and Mermin N D 1976 *Solid State Physics* (Brooks/Cole, Thomson Learning, USA) chap. 8
- [2] Griffiths D J and Steinke C A 2001 *Am. J. Phys.* **69** 137
- [3] Pacher C, Rauch C, Strasser G, Gornik E, Elsholz F, Wacker A, Kießlich G and Schöll E 2001 *App. Phys. Lett.* **79** 1486
- [4] Morozov G V, Sprung D W L and Martorell J 2002 *J. Phys. D: Appl. Phys.* **35** 2091
- [5] Morozov G V, Sprung D W L and Martorell J 2002 *J. Phys. D: Appl. Phys.* **35** 3052
- [6] Courtade E, Houde O, Clément J F, Verkerk P and Hennequin D 2006 *Phys. Rev. A* **74** 031403(R)
- [7] Ponomarev A V, Madroñero J, Kolovsky A R and Buchleitner A 2006 *Phys. Rev. Lett.* **96** 050404
- [8] Wang T, Javanainen J and Yelin S F 2007 *Phys. Rev. A* **76** 011601(R)
- [9] Olson S E, Terraciano M L, Bashkansky M and Fatemi F K 2007 *Phys. Rev. A* **76** 061404(R)
- [10] Houston N, Riis E and Arnold A S 2008 *J. Phys. B: At. Mol. Opt. Phys.* **41**, 211001
- [11] Reyes J A and Lakhtakia A 2006 *Optics Comm.* **259**, 164
- [12] Luna-Acosta G A, Schanze H, Kuhl U and Stöckmann H J 2008 *New J. Phys.* **10** 043005
- [13] Lipson R H and Lu C 2009 *Eur. J. Phys.* **30** S33
- [14] Estevez J O, Arriaga J, Méndez Blas A and Agarwal V 2009 *Appl. Phys. Lett.* **94** 061914
- [15] Archuleta-Garcia R, Moctezuma-Enriquez D and Manzanares-Martinez J 2010 *J. of Electromagn. Waves and Appl.* **24** 351
- [16] Vasseur J O, Hladky-Hennion A-C, Djafari-Rouhani B, Duval F, Dubus B, Pennec Y and Deymier P A 2007 *J. Appl. Phys.* **10** 114904
- [17] Vasseur J O, Deymier P A, Djafari-Rouhani B and Pennec Y 2008 *Phys. Rev. B* **77** 085415
- [18] Sigalas M M and Economou E N 1994 *J. Appl. Phys.* **75** 2845
- [19] Morales A, Flores J, Gutiérrez L and Méndez-Sánchez R A 2002 *J. Acoust. Soc. Am.* **112** 1961
- [20] Sánchez-Pérez J V, Caballero D, Martínez-Sala R, Rubio C, Sánchez-Dehesa J, Meseguer F, Llinares J and Gálvez F 1998 *Phys. Rev. Lett.* **80** 5325
- [21] Kouwenhoven L P, Hekking F W J, van Wees B J, Harmans C J P M, Timmering C E and Foxon C T 1990 *Phys. Rev. Lett.* **65** 361
- [22] Sprung D W L, Wu H and Martorell J 1993 *Am. J. Phys.* **61** 1118
- [23] Pereyra P 1998 *Phys. Rev. Lett.* **80** 2667
- [24] Exner P, Tater M and Vaněk D 2001 *J. Math. Phys.* **42** 4050
- [25] Martínez-Mares M and Robledo A 2009 *Phys. Rev. E* **80** 045201(R)
- [26] Yu Jiang, Martínez-Mares M, Castaño E and Robledo A 2012 *Phys. Rev. E* **85** 057202
- [27] Lee P A and Ramakrishnan T V 1985 *Rev. Mod. Phys.* **57** 287
- [28] Mello P A and Kumar N 2005 *Quantum Transport in Mesoscopic Systems: Complexity and Statistical Fluctuations* (Oxford University Press, New York) p 53.
- [29] Wolf A, Swift J B, Swinney H L and Vastano J A 1985 *Physica D* **16** 285

- [30] Merzbacher E 1998 *Quantum Mechanics* (John Wiley & Sons, Inc.), third edition, p 101
- [31] Kronig R de L and Penney W G 1931 *Proc. R. Soc. London Series A* **130** 499
- [32] Heiligenthal S, Dahms T, Yanchuk S, Jüngling T, Flunkert V, Kanter I, Schöll E and Kinzel W 2011 *Phys. Rev. Lett.* **107** 234102
- [33] Geisel T 1984 *Phys. Rev. Lett.* **52** 1936
- [34] Baldovin F and Robledo A 2002 *Europhys. Lett.* **60** 518
- [35] Mello P A 1988 *Phys. Rev. Lett.* **60** 1089
- [36] Mello P A and Stone A D 1991 *Phys. Rev. B* **44** 1089
- [37] Esaki L and Tsu R 1970 *IBM J. Res. Dev.* **14** 61